ELSEVIER

Seminars in
NUCLEAR
MEDICINE

Determination of Age-Related Changes in Structure and Function of Skin, Adipose Tissue, and Skeletal Muscle With Computed Tomography, Magnetic Resonance Imaging, and Positron Emission Tomography

Natasha E. Wehrli, BSc, Gonca Bural, MD, Mohamed Houseni, MD, Khaled Alkhawaldeh, MD, Abass Alavi, MD, and Drew A. Torigian, MD, MA

In this article, we report quantitative preliminary data obtained from retrospective analysis of ^{18}F-fluorodeoxyglucose positron emission tomography (FDG-PET) and combined PET–computed tomography (PET/CT) examinations in subjects ages 3 to 84 years pertaining to changes in the metabolism of skin, subcutaneous adipose tissue, visceral adipose tissue, and skeletal muscle with age, as well as age-related changes in skeletal muscle attenuation. We also propose a new method for identifying hypermetabolic brown fat on FDG-PET. Finally, we present a review of the literature regarding reported age-related structural and functional changes that occur in skin, fat, and skeletal muscle. Using FDG-PET, We evaluated 213 subjects for changes in the metabolism of skin, adipose tissue, and skeletal muscle with aging. Thirty-two separate subjects were chosen to measure maximum standardized uptake value (SUV) of hypermetabolic brown fat on dual-time point PET imaging. Finally, 15 subjects evaluated by PET/CT were selected to measure changes in metabolism and attenuation of skeletal muscle, and changes in metabolism of adipose tissue with aging. We found that skin, fat, and skeletal muscle all demonstrate significant ($P < 0.05$) increases in SUV with increasing age on PET imaging. Dual-time point PET imaging demonstrates increasing FDG uptake of hypermetabolic brown fat in various regions studied. Finally, our PET/CT studies revealed statistically insignificant ($P > 0.05$) decreases in SUV of adipose tissue with aging and the opposite trend in skeletal muscles ($P > 0.05$). Skeletal muscle attenuation in the various regions studied was found to significantly decrease with age ($P < 0.05$). Our study shows notable trends in metabolism and attenuation of skeletal muscle and metabolism of skin and adipose tissue that occur with normal aging. We hope that the methodologies and data we present here will serve as a useful starting point for those interested in conducting future prospective research on age-related changes in these structures.
Semin Nucl Med 37:195-205

Currently, there are few published data reporting normal changes in structure or function of skin, adipose tissue, and skeletal muscle associated with aging. Techniques such as immunohistochemistry, laser Doppler flowmetry, laser Doppler velocimetry, photoplethysmography, and intravital capillaroscopy all have been used to gather information about the changing composition of the epidermis and dermis as well as the vascular supply to these structures during the aging process. Nevertheless, studies have yielded conflicting data, and many have been inconclusive regarding normal structural changes that occur with aging.[1]

Investigations evaluating changes in fat distribution and metabolism with aging have likewise been performed. However, many of these studies describe changes in obese subjects with type II diabetes mellitus (DM) rather than normal changes that occur in the absence of these pathologies.[2-4]

Department of Radiology, University of Pennsylvania School of Medicine, Philadelphia, PA.

Address reprint requests to Drew A. Torigian, MD, MA, Department of Radiology, Hospital of the University of Pennsylvania, 3400 Spruce Street, Philadelphia, PA 19104-4283. E-mail: Drew.Torigian@uphs.upenn.edu

0001-2998/07/$-see front matter
doi:10.1053/j.semnuclmed.2007.02.002

There have been several studies used to investigate changes in skeletal muscle volume, composition, and blood supply with aging. However, many of these studies lack imaging data to support their analysis, and those that do often do not compare observations in different age groups.[5-7] Quantitative anatomic and metabolic imaging of these structures in men and women of different ages and racial groups may therefore provide normative data that can help one to distinguish the expected changes related to aging from those caused by pathology, although the spectrum of normal changes and pathologic changes may sometimes overlap. Furthermore, quantitative imaging of structure and function may potentially produce a more reproducible assessment in clinical and research settings when compared with qualitative assessment.

In this article, we report quantitative preliminary data obtained from the retrospective analysis of ^{18}F-fluorodeoxyglucose (FDG) positron emission tomography (PET) and PET/computed tomography (CT) examinations of the chest, abdomen and pelvis in subjects ages 3 to 84 years to measure changes in metabolism of skin, subcutaneous fat and visceral fat, and changes in attenuation and metabolism of various skeletal muscles with aging. We also present a new technique for identifying brown adipose tissue using FDG-PET. Finally, we review the literature regarding what is considered normal structural and functional evolution in these structures with aging throughout a typical lifespan.

Materials and Methods

Institutional review board approval for retrospective data collection and image analysis along with a HIPAA waiver were obtained from the Hospital of the University of Pennsylvania's and the Children's Hospital of Philadelphia's Institutional Review Board before study initiation.

Study Samples and CT and PET Scanning Techniques

PET

A total of 179 subjects (age range, 3-84 years, 88 men, 91 women, 116 white, 63 black) who had FDG-PET scans at the Hospital of the University of Pennsylvania (HUP) and who did not have any evidence of skin diseases were retrospectively included in the skin portion of our study. Another subset of 32 subjects were retrospectively selected for the study of brown fat (age range, 8-72 years, 14 men, 18 women) who had hypermetabolic brown fat activity on FDG-PET imaging confirmed by CT scanning. Subjects with greater FDG uptake in brown fat than in the mediastinal blood pool on attenuation-corrected PET images were selected for this study. Subjects with infiltrated injection sites, increased FDG uptake secondary to primary malignancies, or vascular or nodal abnormalities were excluded. A third subset of 34 subjects (age range, 3-80 years, 15 men, 19 women) who had at least one FDG-PET scan at HUP during 2005 to 2006 was retrospectively selected for the subcutaneous fat study. The PET scans were most commonly performed for current or previous malignancy, but all subjects with disease processes involving the abdominal wall or retroperitoneum were excluded. Subjects who had received radioiodine treatment for thyroid cancer more than 6 months before PET scanning were included if no morphologic abnormalities were observed on the previous CT scan.

PET was performed on a dedicated whole-body scanner (Allegro; Philips Medical Systems, Bothell, WA, or C-PET; ADAC UGM Medical Systems, Milpitas, CA). All subjects fasted for at least 4 hours to ensure a serum glucose level $<$150 mg/dL at the time of injection. After tracer injection, subjects rested on a comfortable chair during the FDG uptake period. PET was initiated 60 minutes after the administration of 140 μCi/kg (5.2 MBq/kg) of FDG through an intravenous indwelling catheter inserted into an antecubital vein. Sequential overlapping scans were acquired from the base of the skull to the mid-thigh, including the neck, chest, abdomen, and pelvis. Transmission scans using a ^{137}Cs point source were interleaved between the multiple emission scans to correct for nonuniform attenuation. The images were reconstructed using an iterative reconstruction algorithm, and both attenuation-corrected and nonattenuation-corrected images were used.

In the portion of the study dedicated to the measurement of brown fat, all subjects underwent FDG-PET scanning and CT scanning on different occasions, with time intervals ranging from 0 to 18 days with a mean of 8 $\pm$ 6 days. Image acquisition for the whole-body PET scans started at a mean time point of 60 minutes after injection of 68 μCi/kg (2.5 MBq/kg) of FDG. This first scan (scan 1) after FDG injection covered the neck, thorax, abdomen, pelvis, and upper thighs and consisted of 4 to 5 emission frames of 25.6-cm length with an overlap of 12.8 cm covering a craniocaudal length of 64 to 76.8 cm. A second emission scan (scan 2) was acquired at a mean time of 110 minutes after tracer injection (range, 100-120 minutes). A transmission scan was obtained with both sets of images for attenuation correction. Image reconstruction was performed with an iterative ordered-subsets expectation maximization algorithm with 4 iterations and 8 subsets. Attenuation-corrected images were obtained by applying transmission maps, which were acquired after FDG injection with a ^{137}Cs source interleaved with the emissions scans.

Five pediatric subjects (4 male, 1 female) 3 to 8 years of age who had a minimum of 1 PET scan at the Children's Hospital of Philadelphia during 2004 to 2006 also were included in the subcutaneous fat analysis. The PET scans were most commonly performed for current or previous malignancy, but all subjects with a current or previous history of any abdominal wall or retroperitoneal involvement were excluded.

PET was performed in pediatric subjects with a dedicated whole-body PET scanner (Allegro; Philips Medical Systems, Bothell, WA, or C-PET; ADAC UGM Medical Systems, Milpitas, CA). All subjects fasted for at least 4 hours, and serum glucose levels were $<$140 mg/dL in all subjects. All were asked to empty their bladders immediately before being scanned. No specific preparation was given to the subjects. PET was initiated 60 minutes after the intravenous adminis-

tration of a dose of FDG adjusted to the body weight (130 μCi/kg (4.8 MBq/kg) for the Allegro and 68 μCi/kg (2.5 MBq/kg) for the ADAC camera). Sequential overlapping scans were acquired to cover from the base of the skull to the mid-thighs, including the neck, chest, abdomen, and pelvis. Transmission scans obtained with a ^{137}Cs point source were interleaved between the multiple emission scans to correct for nonuniform attenuation. The images were reconstructed with an iterative reconstruction algorithm, and both attenuation-corrected and nonattenuation-corrected images were used.

PET/CT

Fifteen subjects (age range, 14-83 years, 7 men, 8 women) had PET-CT scans performed at HUP in April through October of 2006. These studies were chosen to evaluate subcutaneous and visceral fat standardized uptake value (SUV), skeletal muscle SUV, and skeletal muscle attenuation in different age groups. Subjects retrospectively included in the study were those without any evidence of abdominal wall or retroperitoneal pathology and who had received no chemotherapy in the 3 months before the imaging study. PET/CT imaging was initiated using a 16-detector row LYSO PET-CT (Gemini TF; Philips Medical Systems, Bothell, WA). A scout image was initially obtained for subject localization. Whole-body CT axial images were obtained using a low-dose protocol (50-10 mAs) with a 5-mm slice thickness after the administration of oral contrast material. Subsequently, 3D PET data were acquired using 3-minute table positions. The PET acquisition included a time-of-flight and a dead-time correction as well as online delayed coincidence subtraction to correct for random coincidences. Rescaled CT images were used to produce attenuation correction values for the PET emission reconstruction.

Image Analysis

PET SUV Measurement

The maximum skin SUV (SUV_{max}) was measured by placing multiple regions of interest (ROIs) on axial slices about the skin of the posterior thorax, anterior abdomen, and posterior pelvis. In the chest, ROIs were placed on the skin and soft tissue of the posterior thorax through 5 slices passing through the mid-heart. In the abdomen, ROIs were placed on the anterior abdominal skin extending on the 5 consecutive axial slices originating from the lower edge of the liver. In the pelvis, ROIs were placed on the skin of the posterior pelvic wall through all slices involving iliac bone marrow. Computer generated mean SUVs representing the background activity for these regions were also noted.

In the subset of subjects included in the brown fat portion of the study, visual analysis of FDG-PET scans and CT scans of the corresponding areas were used to confirm the diagnosis of hypermetabolic brown fat. Maximum SUVs from 120 hypermetabolic brown fat foci were analyzed in standard fashion. SUV_{max} was calculated at the first time point and the second time point from axial images by placing ROIs around brown fat accumulations.

SUVs of the subcutaneous fat in the back and abdomen were obtained on FDG-PET and PET/CT scans by placing a 2-cm^2 ROI on axial images at the level of the inferior pole of the right kidney in each subject. SUVs were measured in the abdominal subcutaneous fat at a point extending halfway from the midline to the midaxillary line bilaterally and in the regions of subcutaneous fat of the back directly posterior to the original ROIs on the same axial plane. Computer-generated maximum SUVs were recorded and averaged between the 4 sites for each subject.

SUVs of the visceral fat in the left and right retroperitoneal regions were obtained on PET and PET/CT scans by placing a 2-cm^2 ROI on axial slices directly below the inferior pole of each kidney. Computer-generated maximum SUVs were recorded and averaged between the 2 measured sites for each subject. In the separate measurements of brown fat, maximum SUVs for 120 different locations between the 2 time points were measured, and the average percent change was calculated and recorded for each location.

SUVs of skeletal muscle were obtained on PET/CT scans in 3 separate regions. A 2-cm^2 ROI was placed in the center of the psoas muscle on an axial plane inferior to both kidneys. Another 2-cm^2 ROI was selected to measure subscapularis SUV at the midportion of the muscle on an axial slice directly inferior to the scapular spine bilaterally. A third 2-cm^2 ROI of the infraspinatus SUV was measured on the same axial plans as those chosen for measurements of subscapularis muscles. Computer generated maximum SUVs were recorded and averaged between the two sites for each muscle in each subject.

CT Attenuation Measurement

Muscle attenuation values (measured in Hounsfield units [HU]) were obtained from unenhanced whole-body PET/CT scans in the following manner: 2-cm^2 ROIs were manually placed in the midportion of the psoas muscle inferior to the kidneys bilaterally, in the midportion of the subscapularis muscle anterior to the scapulae bilaterally, and in the midportion of the infraspinatus muscle posterior to the scapulae on the same axial slices as the subscapularis muscle. Average attenuation values for these ROIs were measured, and the average between the 2 sites was recorded for each subject.

Data Analysis

Partial volume correction was applied to generate corrected skin SUVs as described in the literature. Skin thickness was measured from CT images in the thorax, abdomen, and pelvis, and the values were averaged to 5 mm in all of these regions in all subjects. Partial volume corrected SUV_{max} of skin was then calculated using the following formula: Corrected SUV_{max} = ([measured SUV_{max} of skin – background SUV_{mean} of skin]/recovery coefficient [RC] + background SUV_{mean} of skin), where the RC for skin thickness was based on the sphere recovery function data for PET reported by Lubberink and coworkers.[8]

By using this mathematical formula, we were able to calculate the partial volume corrected SUV_{max} for the skin on each axial slice. We then summed these corrected skin SUVs from 5 axial slices in the posterior thoracic region and averaged them. We then repeated this procedure in the anterior

Table 1 Skin SUV_{max} on FDG-PET in Different Racial Groups

	Skin SUV in White Subjects	Skin SUV in Black Subjects	*P* Value
Posterior thorax	3.8 ± 1.0	4.2 ± 1.0	0.05
Anterior abdomen	2.8 ± 1.0	3.4 ± 1.0	0.004
Posterior pelvis	3.1 ± 1.2	3.7 ± 1.1	0.001

abdomen and posterior pelvis and calculated the average corrected SUV_{max} for each of these regions in each individual subject. Analyses of the partial volume corrected SUV_{max} of skin were subsequently performed to assess for changes with age, gender, race, and anatomic site as noted previously.

Average corrected SUVs of the subcutaneous fat, visceral fat, and skeletal muscle in various regions were correlated with the age of each subject. Mean skeletal muscle attenuation in all subjects also was correlated with age. All scatterplots were performed with Microsoft Excel software (Microsoft Corp, Redmond, WA). Linear regression curves and statistical analyses were performed with SPSS version 14.0 (SPSS Inc, Chicago, IL). Pearson *r* correlation values and two-tailed p values were calculated, and statistical significance was considered to be present for *P* values <0.05.

Results

After partial volume correction, the maximum skin SUVs ranged between 1.35 and 6.75. The maximum skin SUVs for 3 different body regions were greater in the black population than in the white population ($P < 0.05$; Table 1). Maximum SUV measurements increased with age in the white population ($P < 0.05$) in all regions studied. A trend of increasing maximum SUV values with age did not reach statistical significance in the black population ($P > 0.5$). There were no statistically significant differences in corrected SUV measurements for any region between both genders. Data regarding skin SUVs for the 3 ROIs in both genders and both racial groups are provided in Table 2. Figures 1 and 2 contain data with the average partial volume corrected maximum SUVs of skin from all anatomic sites studied in white and black subjects, respectively.

Hypermetabolic brown fat, as demonstrated by increased FDG uptake on PET, was identified in 32 subjects and confirmed by CT in the supraclavicular region, axillae, cervical region, paravertebral area, mediastinum, and upper abdomen. Hypermetabolic brown fat was confined to the supraclavicular region in 6 subjects (4 adults older than the age of 30 years and 2 subjects younger than the age of 16 years). The other 26 subjects demonstrated a combination of 2 or more sites with hypermetabolic brown fat. Table 3 shows the body distribution of hypermetabolic brown fat in 32 subjects.

Table 2 Skin SUV_{max} on FDG-PET of Male and Female Subjects of Different Racial Groups

	Skin SUV in Males	Skin SUV in Females	*P* Value
White subjects			
Posterior thorax	3.8 ± 1.1	3.9 ± 0.9	>0.05
Anterior abdomen	2.8 ± 1.1	2.8 ± 1.0	>0.05
Posterior pelvis	3.2 ± 1.2	2.9 ± 1.2	>0.05
Black subjects			
Posterior thorax	4.3 ± 1.1	4.0 ± 1.5	>0.05
Anterior abdomen	3.2 ± 1.0	3.4 ± 1.0	>0.05
Posterior pelvis	3.2 ± 1.0	3.9 ± 1.0	0.02

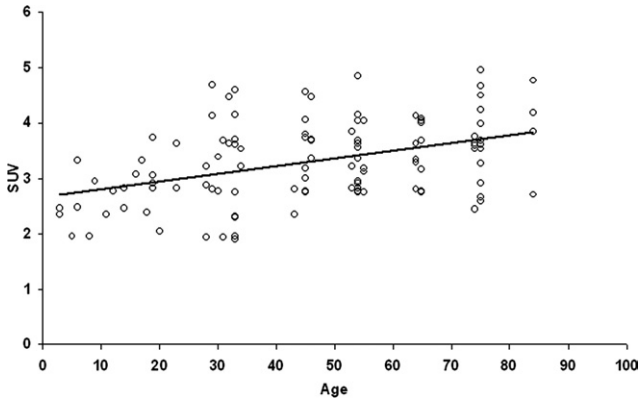

Figure 1 Average partial volume corrected SUV_{max} of skin at all anatomic regions on FDG-PET in white subjects versus age.

Table 4 shows brown fat SUV_{max} in different body locations and % SUV_{max} change on dual-time point scanning. On dual-time point imaging, there was a significant change in the SUV of brown fat; 91 (76%) of the brown fat foci demonstrated an increase in SUV_{max}. The percent increase ranged from 12% to 192%, with a mean value of 42 ± 40%. Sixteen (13%) of the brown fat foci did not show any change, whereas 11 (11%) of the brown fat foci showed a decrease in SUV_{max} by 4 to 12%. There was an increase in the number of hypermetabolic brown fat foci in 3 subjects on the second time point images, occurring in the supraclavicular, mediastinal and paravertebral regions. Although symmetric in distribution, there was significant variability in SUV_{max} between the 2 sides of the body, ranging from 0% to 42% with a mean value of 21 ± 11% ($P < 0.05$).

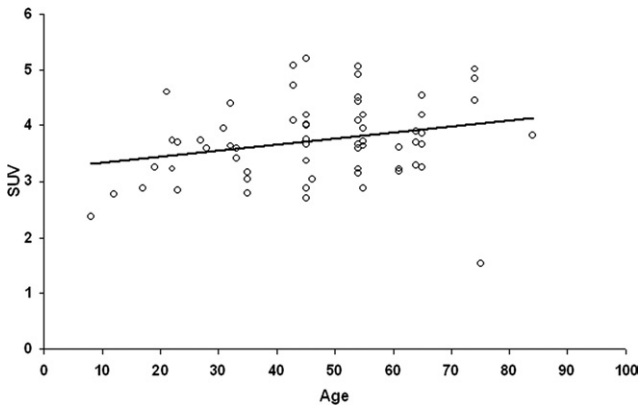

Figure 2 Average partial volume corrected SUV_{max} of skin at all anatomic regions on FDG-PET in black subjects versus age.

Table 3 Anatomic Distribution of Hypermetabolic Brown Fat on FDG-PET

Brown Fat Site	No. of Subjects
Supraclavicular area	7
Supraclavicular area + cervical	5
Supraclavicular area + cervical + axillae	5
Supraclavicular + cervical + paravertebral + axillae	9
Supraclavicular + cervical + paravertebral + axillae + mediastinum	4
Supraclavicular + cervical + paravertebral + axillae + upper abdomen	2
Mediastinum alone	0
Upper abdomen alone	0

Average subcutaneous fat SUV was found to increase with increasing age in PET subjects ($r = 0.62$, $P < 0.05$). Average subcutaneous fat SUV decreased slightly over time in subjects who underwent PET/CT, although these findings were without statistical significance ($r = -0.29$, $P = 0.83$). Average perirenal fat SUV also was found to increase with increasing age in PET subjects ($r = 0.47$, $P < 0.05$). The opposite trend was found in PET-CT subjects, but this trend was not found to be statistically significant ($r = -0.22$, $P = 0.42$).

Average psoas muscle and infraspinatus muscle attenuations in PET/CT subjects were found to significantly decrease with age (psoas: $r = -0.83$, $P < 0.05$; infraspinatus: $r = -0.63$, $P < 0.05$) whereas subscapularis attenuation showed a similar pattern although without statistical significance ($r = -0.48$, $P = 0.07$). Average psoas, subscapularis, and infraspinatus muscle SUVs in PET/CT subjects showed an increasing trend with age, although none of these findings were statistically significant (psoas: $r = 0.39$, $P = 0.14$; subscapularis: $r = 0.43$, $P = 0.11$; infraspinatus: $r = 0.26$, $P = 0.35$).

Figures 3 and 4 are scatterplots of subcutaneous fat and perirenal fat SUV_{max} measured from FDG-PET images correlated to subject age, respectively. Figure 5 shows SUV_{max} versus age in the psoas muscle measured from PET/CT images, and Figure 6 shows the correlation between psoas muscle attenuation with age as measured on PET/CT studies.

Table 4 Maximum SUV and Dual-Time Point FDG-PET Data for Hypermetabolic Brown Fat in Different Anatomic Regions

Brown Fat Area	Range (Mean) of SUV_{max}	% Change on Dual-Time Point Scanning
Supraclavicular	2.4-12.4 (7.2)	−12-192%
Cervical	2.3-7 (5.2)	−15-110%
Axillary	2.5-5 (4.2)	−8-60%
Paravertebral	0.9-4.1 (3.1)	−20-40%
Mediastinal	2.5-7 (4.7)	−10-70%
Upper abdominal	2.9-3.8 (3.2)	0-35%

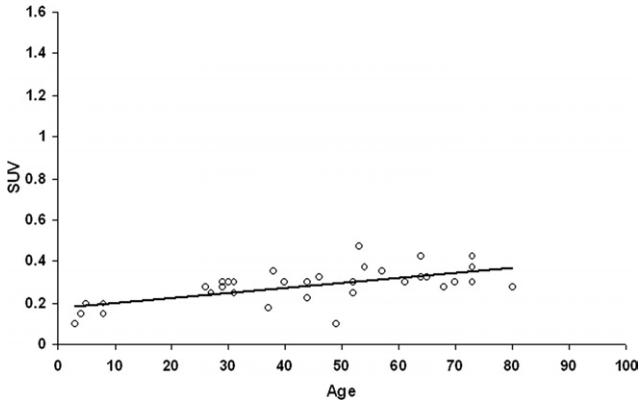

Figure 3 Subcutaneous fat SUV_{max} on FDG-PET versus age.

Discussion

Changes in Structure and Function of the Skin With Aging

Aging is a complex, multifactorial process resulting in structural and functional changes in the skin. These changes result from intrinsic and extrinsic processes, such as exposure to ultraviolet (UV) radiation. Recent advances in skin biology have increased our understanding of skin homeostasis and the aging process, as well as the mechanisms by which UV radiation contribute to photoaging and cutaneous disease.[9]

Two types of aging, chronological skin aging and photoaging, have distinct clinical and histological features. Chronological skin aging is a universal and inevitable process characterized primarily by physiologic alterations in skin function. In this case, keratinocytes are unable to properly terminally differentiate to form a functional stratum corneum, and the rate of formation of neutral lipids that contribute to the barrier function slows, leading to dry pale skin with fine wrinkles. In contrast, photoaging results from exposure to solar UV radiation, leading to premature aging of the skin, and the damage thus becomes apparent in sun-exposed skin.[10] Photoaging is a cumulative process that occurs based on the degree of sun exposure and the amount of pigment in the skin. UV irradiation induces matrix metalloproteinases (MMPs) responsible for alterations in the collag-

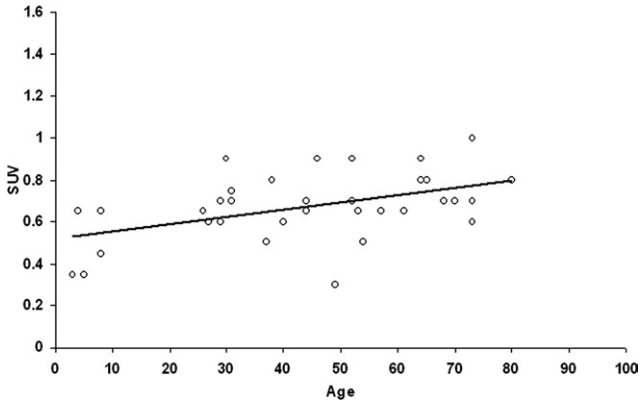

Figure 4 Perirenal fat SUV_{max} on FDG-PET versus age.

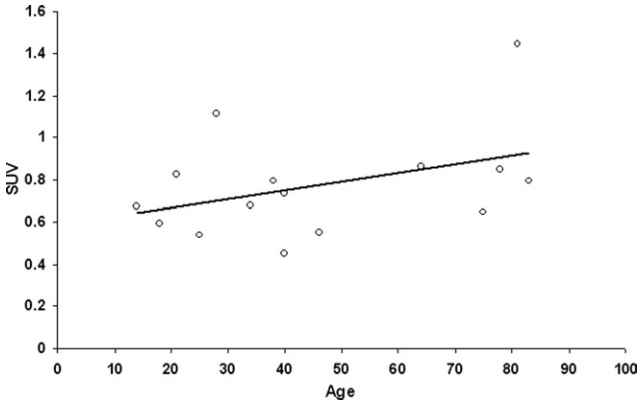

Figure 5 Psoas muscle SUV_{max} on FDG-PET/CT versus age.

enous extracellular matrix of dermal connective tissue, and the cumulative activity of these enzymes impairs the integrity of skin. Clinically, it is characterized by wrinkles, mottled skin pigmentation, roughening of the skin, and loss of skin tone.[11] On a molecular level, UV radiation from the sun alters keratinocytes and fibroblasts, resulting in the activation of cell surface receptors that initiate signal transduction cascades. This in turn leads to a breakdown of collagen in the extracellular matrix, and a shutdown of new collagen synthesis.[12]

Racial variability in skin anatomy and function is a popular area of study. Understanding normal racial differences in skin appearance and function is important in identifying and treating disease states in subjects of different racial backgrounds. The interpretation of ethnic differences in skin properties should consider not only anatomic and functional characteristics but also socioeconomic, hygienic, and nutritional factors.[13] It has been reported that African skin has the largest quantity of melanin per milligram of epidermis in both photoexposed and unexposed regions. This trend was followed in turn by Indian, Mexican, Chinese, and European white skin. It was also found that the size of melanosomes was greatest in the African subjects and smallest in the European white subjects. Therefore, genetic differences in skin composition play a large role in ethnic differences in appearance and function of skin, irrespective of environmental influences.[9,14]

Many tools have been used to better determine changes that occur in perfusion, pH, histologic appearance, and overall thickness of skin over time. They include microscopy, laser Doppler flowmetry, laser Doppler velocimetry, photoplethysmography, and intravital capillaroscopy. Several studies using these tools have suggested that aging may be associated with decreased cutaneous perfusion, particularly in photo-exposed areas,[15,16] although future studies with more subjects would be helpful in better clarifying this trend. Evaluation of skin pH has shown that it tends to remain relatively constant from childhood through to the age of 70 years, and then rises precipitously, particularly in the lower limbs. This increase in skin pH is believed to be caused by stasis and reduced oxygen supply in older individuals. Some concern has been raised, however, that techniques used to measure pH from biopsy specimens may provide falsely elevated values.[17,18]

Ultrasonographic, immunohistologic, and electron microscopy studies of skin have demonstrated retraction of the epidermal papillae, leading to a flattening of the dermal/epidermal junction with age. In young skin, basal cells send numerous villous cytoplasmic projections into the dermis, giving the appearance of a tortuous dermal/epidermal junction. This typically continues until the sixth decade of life, at which time flattening at this junction begins to occur. This tendency toward flattening may cause aged skin to be less resistant to shearing forces. In addition, aged epidermis may demonstrate decreased proliferative potential and reduced absorptive capacity.[19-21]

Studies of epidermal thickness have been somewhat inconclusive. One investigation in 34 women ages 18 to 69 years revealed an overall thinning of live epidermis on the back of the arm with increasing age,[22] whereas another that examined changes in the dorsal forearm, buttock, and shoulder region in 71 people ages 20 to 68 years found no significant change in epidermal thickness with age. These investigators did, however, note a positive correlation between skin thickness, pigmentation, and blood content. Moreover, nonsmokers and male subjects also demonstrated a thicker stratum corneum (the most superficial layer of epidermis composed of dead flat keratinocytes) when compared with smokers and women.[23]

Our current study evaluates the changes in metabolic activity in skin in both white and black subjects. SUV_{max} of skin from various regions of the body increases with age in both ethnic groups. Because subjects were not questioned about degrees of past sun exposure, these findings may be reflective of the influences of extrinsic factors such as UV radiation or intrinsic processes, although it is unclear as to what degree each of these processes has played a role in each particular subject. UV radiation leads to more neutrophil activity in the dermis with subsequent release of free radicals, MMPs, and impaired collagen production.[12] Chronologic aging, although less well understood, is also believed to be caused by cumulative oxidative stress, increased activity of MMPs, and breakdown of collagen production. Increasing inflammatory activity and turnover of keratinocytes and other cells that

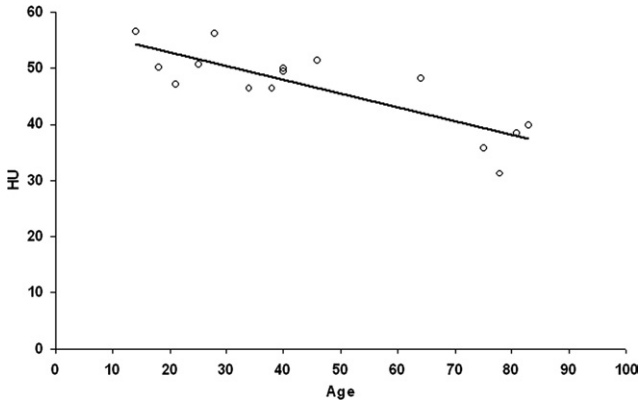

Figure 6 Psoas muscle attenuation on FDG-PET/CT versus age.

reside in the epidermis and dermis may both, therefore, be responsible for the observed increase in metabolic activity in our study populations with age.

In the black population, where there is a greater proportion of melanin in the dermis, this trend appears to be less pronounced. These findings support the notion that increasing levels of pigment in the dermis attenuate UV penetration, thereby reducing the amount of free radicals, number of degradative proteins, and ultimately the degree of inflammatory activity that occurs in the skin with photoaging.[13] Although darker-skinned individuals demonstrate less of a response to UV radiation, they likely still experience oxidative damage from chronological aging and, therefore, metabolic activity of the skin would still be expected to increase with age, just not to the same extent as in lighter-skinned subjects. This concept may explain why black subjects in our study showed a positive correlation of SUV_{max} of skin with aging, although not to the same degree as that of the white subjects we evaluated.

This portion of our study was limited in that it was retrospective in nature with a potential for sampling error. In addition, we did not have any information about previous sun exposure, which may have influenced the degree of metabolic activity in some of our study subjects. We also did not inquire about use of medications, smoking status, and other demographic factors that could have influenced our findings. In the future, it may be useful to conduct a prospective, longitudinal study where degree of sun exposure and other demographic information is available to demonstrate changes that occur in skin metabolism over time and to assess how much of those changes are due to natural aging processes versus other contributing factors.

Changes in Structure and Function of Adipose Tissue With Aging

White and brown adipose tissues represent counter players in the balance of energy metabolism. The main function of white adipocytes is to store excess energy in lipid form, which is then mobilized to other tissues in response to metabolic needs, especially in times of decreased caloric intake. Brown adipocytes use accumulated lipids obtained from ingested food as a source of chemical energy that can be released from cells in the form of heat.[24] White adipose tissue can be subdivided into subcutaneous fat, located beneath the dermis throughout the body, intramuscular fat, surrounding skeletal muscle fiber bundles, and visceral fat, encasing various organs deep to the body wall of the chest, abdomen and pelvis. These different locations of white adipose tissue are distinguishable by cross-sectional imaging using CT or magnetic resonance imaging (MRI).[25]

Brown Adipose Tissue

Brown adipose tissue plays an important role in cold-induced and diet-induced thermogenesis.[26] The brown color is attributed to high vascularity and mitochondrial density. The mitochondria in brown adipose tissue exclusively express the thermogenic protein responsible for uncoupling respiration from adenosine triphosphate synthesis, leading to the dissipation of heat. FDG uptake in hypermetabolic brown fat on PET imaging occurs as glucose transporters are abundant in brown adipose tissue.[27]

FDG uptake in the neck and shoulders have been observed on whole-body PET for many years and used to be attributed to muscle activity, particularly because this uptake usually resolved after the administration of a benzodiazepine, a muscle relaxant.[28] However, combined PET/CT images subsequently revealed that, in some patients, these foci of FDG uptake were localized to adipose tissue rather than to muscle.

In the fetus and neonate, brown adipose tissue is abundant because it serves an important role in thermoregulation, and diminishes with increasing age because of reduced demands for thermogenesis.[29,30] Our study did not include data about the prevalence of brown fat, but the age distribution of our study group demonstrates that hypermetabolic brown fat is more commonly found in children than in adults. The literature also reports that FDG uptake in brown fat is more common in women than in men,[31,32] which is consistent with the female to male ratio in our study group of 19:13.

In our study, brown fat was distributed throughout the cervical, supraclavicular, axillary, paravertebral, mediastinal, and upper abdominal regions, which is similar to what has been reported previously. This distribution serves as a warming mechanism for the blood supply of vital organs, where cervical fat corresponds to the vascular supply of the head and neck, paravertebral fat corresponds to the spinal cord vascular supply, mediastinal and pericardial fat protect the heart and great vessels, and perirenal fat surrounds the kidneys.[29]

Our investigation revealed that hypermetabolic brown fat in the mediastinum and upper abdomen was always associated with FDG uptake in brown fat in the more typical locations (supraclavicular, paravertebral, and axillary regions), and that this distribution is comparable with what has been previously reported.[29,33-35] Increased FDG uptake in brown adipose tissue in the neck can lead to a false-positive result of malignancy in 2.3% to 4% of patients[31,32]; however, in our study, there were no cases of cervical brown fat that were misinterpreted as malignancy. Typically, the increased FDG uptake in brown fat in the cervical, supraclavicular, axillary, and paravertebral regions is bilateral and symmetric and is seldom confused with malignancy. However, hypermetabolic brown fat in the mediastinum and upper abdomen are more likely to be misinterpreted as a primary malignancy or nodal metastases due to its unusual location and frequently asymmetric distribution.[28,29,36] In our study, 6 subjects (19% total) had hypermetabolic brown fat in the mediastinum and upper abdomen, and in 3 of these subjects, increased FDG uptake in these locations was misinterpreted as nodal metastases on PET images alone but correctly interpreted when correlation with CT images was performed.

Dual-time point FDG-PET imaging has been reported to be a useful technique to help one discriminate between benign and malignant disease, with images obtained at 2 sequential time points after the administration of FDG. Hustinx and coworkers used dual-time point imaging for head and

neck tumors and demonstrated improved separation of malignant lesions from inflamed sites.[35] Nakamoto and coworkers found that malignant lesions showed a significant increase in SUV over the course of time and that benign lesions showed a decrease in SUV over the course of time.[37] Lodge and coworkers came to a similar conclusion in a study of 29 patients with various benign and malignant soft-tissue masses.[38] Kumar and coworkers had applied dual-time point imaging in breast cancer and found that breast malignancies show increasing FDG uptake with time, whereas uptake of FDG in inflammatory lesions and normal breast tissues decreases over time.[39]

Matthies and coworkers used dual-time point FDG-PET to evaluate pulmonary nodules and showed that this technique resulted in a very high sensitivity and specificity for detection of malignant lung nodules.[40] Differences in levels of glucose-6-phosphatase and hexokinase within benign and malignant cells have been postulated as the underlying explanation for this phenomenon.[41] However, our study is the first to document changes in SUV_{max} of brown adipose tissue on FDG-PET using a dual-time point imaging technique, and shows that brown adipose tissue is a nonmalignant lesion that tends to have increasing FDG uptake on dual-time point imaging.

The main limitation of this portion of our study is that we examined PET and CT examinations performed at different times rather than using combined PET/CT, which may result in the potential misinterpretation of increased FDG uptake by primary malignancy or nodal disease as hypermetabolic brown fat, as PET/CT has been reported to be superior to visual correlation between separate PET and CT scans.[42,43] Additionally, we did not obtain biopsy confirmation of presumed brown fat in any of our subjects.

White Adipose Tissue

There is minimal published literature that describes the normal changes in adipose tissue with aging, and even fewer reports that discuss changes in fat metabolism in the absence of comorbid conditions such as type II DM. One 10-year longitudinal study performed in subjects ages 48 to 76 years at baseline did report an average of 1.1 kg increase in body weight over the course of 10 years in women and 1.0 kg in men, all of which was attributed to increasing fat mass. The same group of investigators revealed a decrease in overall skin thickness and arm and thigh girth, whereas waist circumference in women and hip circumference in men both increased over time. These findings suggest an overall decrease in subcutaneous fat over time, with possible redistribution to visceral fat, although the main limitation of this study was the lack of imaging data to support these trends.[44]

Several investigations report changes in fat mass as measured by various imaging modalities. A 2-year longitudinal study in 65-year-old African-American women revealed a pattern of increased visceral adiposity as well as increased amounts of intramuscular fat content as determined by full-body MRI and magnetic resonance spectroscopy.[45] A separate study compared gender and racial differences in fat and muscle composition by dual-energy radiograph absorptiometry scanning in subjects ages 70 to 79 years during a 2-year period. There was no detected difference in overall weight gain between racial groups, although men were found to have a greater increases in total fat mass than women, particularly in the adipose content of the trunk and extremities.[46]

Most of the current literature documenting changes in the structure, distribution, volume, and metabolism of adipose tissue is focused on its relevance to obesity and the development of metabolic syndrome. One MRI study performed in a group of 150 subjects demonstrated notable differences in whole-body adipose tissue compartments in men and women as a function of age. All selected subjects had an increased risk of type II DM, but it was determined that there was a strong correlation between percentage of visceral adiposity and age, whereas subcutaneous adiposity remained virtually unchanged in men and only slightly increased in women. Older women also demonstrated a significant increase in intrahepatocellular lipids compared with men, whereas intramyocellular lipid content remained relatively independent of age in both genders.[2] Another study found that both visceral fat and aging are independent risk factors for the development of type II DM.[3] In a third study using FDG-PET and MRI, patients with abdominal obesity showed markedly reduced uptake of glucose in both skeletal muscle and adipose tissue, which was particularly pronounced in men.[4]

Our study is the first to describe changes that occur in fat metabolism in the absence of type II DM. The results were interesting in that SUV_{max} of both subcutaneous and visceral fat measured by FDG-PET alone showed a positive correlation with age, whereas a tendency toward negative correlation was noted when measuring SUV_{max} on PET/CT studies. This discrepancy may be related to an artificial elevation of SUVs on PET images from PET/CT examinations related to the presence of beam hardening artifact from structures such as cortical bone on the CT images that are used for attenuation correction purposes.[47] As such, SUV_{max} measured on PET/CT may be preferentially falsely elevated in younger subjects because of their greater density of bone (with an associated greater amount of beam hardening artifact) when compared with older subjects with less dense bone. We believe that if we were able to correct for this artifact, we would have seen a positive correlation between metabolic activity in both types of white adipose tissue with age, as demonstrated in subjects who had undergone PET imaging alone.

The increase in metabolic activity in visceral and subcutaneous fat with aging may reflect an increase in the body's efficiency in the long-term storage of energy as fat. This is supported by studies that show that weight gain is common as individuals progress through adulthood and beyond.[44] Another potential explanation for this increase in metabolic activity is the redistribution of fat depots to other sites, such as muscle and bone marrow. This phenomenon has been hypothesized to be the result of reduced fat cell size and function and impaired differentiation of preadipocytes into fat cells with aging.[48] If this is the case, the remaining adipocytes in the superficial fascia and surrounding organs become smaller and denser, leading to the misleading measurement

of increasing metabolic activity of these tissues with aging, while individual cells may actually become less active over time as fat depots are redistributed to other regions of the body.

The major limitation of this portion of our study is the small sample size used in our PET/CT measurements, attributable to a limited number of qualifying studies performed at our institution, potentially leading to a selection bias in our results. In addition, limitations in spatial resolution of PET images may have led to sampling errors in our measurements, in particular in the measurements obtained in the perirenal space. Finally, our sample population only included subjects without insulin resistance. Although fat metabolism is likely altered in subjects with insulin resistance, possibly leading to obscuration of some of the above reported changes with normal aging, it would still be useful to conduct future studies to evaluate differences in fat metabolism between diabetic and nondiabetic subjects with increasing age, given the high prevalence of DM.

Changes in Structure and Function of Skeletal Muscle With Aging

Skeletal muscle is one of the most vascular organs in the human body and is also the most dynamic in its ability to substantially increase both blood flow and metabolic rate in response to physiologic challenges.[6] Aging is associated with decrements in microvascular function and exercise tolerance, along with other structural and functional changes that typically begin in the fourth decade of life.[7] In general, it is well established that skeletal muscle mass declines with age and that there is a concomitant loss of muscle strength.[49,50] However, aging may selectively affect different muscles in different ways. In one study, histologic comparisons of human vastus lateralis and masseter muscles in both young adults and the elderly revealed that type I fibers become more circular in the masseter muscle with age but decrease in size in the vastus muscle. Meanwhile, type II fibers decreased only slightly in size in the masseter whereas they became very small in the vastus muscle.[51]

MR, ultrasonographic, and near-infrared spectroscopic techniques have all been used to demonstrate reduced capillary density and maximal blood flow as well as decreased hyperemic flow response in muscle with aging.[52] Decreases in rates of muscle protein synthesis such as of myosin heavy chain and mitochondrial proteins have also been reported. Furthermore, it has been shown that aerobic exercise, resistance exercise, insulin, and certain amino acids all enhance muscle mitochondrial biogenesis and protein synthesis, although severe dysfunction in these mechanisms may occur in patients with type II DM.[7]

Cross-sectional imaging techniques have been used to examine the influence of age on skeletal muscle mass. One 12-year longitudinal study used CT to evaluate changes in skeletal muscle size in 9 healthy sedentary men over time. Significant reductions in the cross-sectional areas of all thigh muscles, including the quadriceps and hamstrings, were noted, and correlations were made to reductions in muscle strength. Muscle biopsies taken at the time of the imaging also demonstrated reductions in type 1 fibers and capillary-to-fiber ratios during the 12-year period.[53] Another study using MRI reported a decrease in skeletal muscle mass beginning in the third decade of life, with a predominant loss of mass in the lower trunk and extremities in both men and women.[54] A third study focused specifically on changes that occur in back muscles and the psoas muscle with aging on MRI. These investigators reported that although paraspinal muscle size uniformly decreased with age, intramuscular fat content increased. Psoas muscle also showed a decline in girth with age, although this was not associated with a corresponding increase in intramuscular fat deposits.[55]

There have also been several studies showing physiologic changes that occur in human muscle during exercise and with insulin stimulation. One study reviewed spectroscopic and diffusion-weighted MR techniques to demonstrate water shifts that occur with increased perfusion in exercising muscle.[56] Another study investigated the uptake of FDG in cardiac and skeletal muscle during various intensities of exercise on PET imaging. These investigators found that skeletal muscle glucose uptake rises in parallel with the intensity of exercise, whereas similar measurements in myocardial tissue revealed an increase in uptake with mild-to-moderate exercise, with eventual tapering and decline of uptake with high-intensity exercise, which suggests that skeletal muscle continually uses glucose as its main substrate, whereas cardiac muscle uses substrates other than glucose when exercise intensity is at its highest.[57]

Metabolic imaging also has been used on a more microscopic level to better delineate individual steps of glucose transport into skeletal muscle in response to insulin stimulation. One group used 3 different tracers, ie, [^{15}O]-H_2O, [^{11}C]-3-O-methyl glucose, and FDG, to contrast differences in glucose delivery, transport, and phosphorylation in 2 different skeletal muscles in lean fasting healthy subjects.[58] Other researchers have investigated the use of PET imaging to determine abnormalities in glucose metabolism in patients with type II DM. One group compared lean, nondiabetic obese and type II diabetic obese individuals and showed a dose–response increase in glucose transport in skeletal muscles of the leg in response to insulin stimulation in both lean and nondiabetic obese groups, although glucose transport was shown to be significantly decreased in the diabetic group. In addition, glucose phosphorylation was found to be significantly impaired in both diabetic and nondiabetic obese subjects.[59]

Despite some published literature using functional and metabolic imaging to study skeletal muscle in different populations, there are no studies comparing differences in skeletal muscle metabolism in different age groups. In our study, we evaluated not only differences in SUV_{max} of various skeletal muscles but also differences in attenuation on PET/CT. It has been described that skeletal muscle becomes less dense with age, a phenomenon that may be secondary to disuse atrophy, gradual changes in fiber type,[51,53] and increasing amounts of intramuscular lipid deposits.[55] In our study, attenuation in every muscle that was evaluated was inversely

correlated with age. Interestingly, SUV_{max} showed the opposite trend, increasing with age. Although decreasing attenuation can be explained by factors already described,[51,53,55] it is unclear as to what would cause an increase in muscle metabolic activity with aging. Of note, none of our subjects had insulin resistance, and we attempted to select muscles that were most likely to be inactive at the time of PET imaging. One theory is that some of these muscles (eg, the psoas muscle) may be in a more constant state of contraction secondary to pain from degenerative joint disease of the thoracolumbar spine. Another possibility is that as the muscles become atrophic with age, the individual fibers and cells become more compact, leading to a falsely elevated measurement of higher metabolic activity, when in actuality metabolic activity is reduced on a cellular level. Future prospective metabolic and other molecular studies may be useful to better elucidate changes that occur on a cellular level in muscle with aging in normal healthy subjects.

The main limitations of this portion of the study were its retrospective nature and the small sample size. In addition, we did not evaluate subjects with type II DM. Further studies with a larger number of subjects may be useful to compare age-related differences in muscle metabolism and attenuation in subjects with and without this condition. It may also be useful to obtain data regarding the level of daily exercise and other factors that may influence muscle use.

Conclusion

Quantitative structural and functional imaging of skin, adipose tissue, and muscle using CT, MRI, and PET may help us better elucidate changes that occur with normal aging processes and provide a normative baseline when assessing patients for the presence of other pathologies. In this article, we reported quantitative preliminary retrospective data obtained from whole-body PET and PET/CT studies regarding changes in attenuation and metabolism of skin, various forms of adipose tissue, and skeletal muscle with age. In addition, we presented a review of the literature regarding reported age-related structural and functional changes that occur in skin, fat, and muscle. We hope that the methodologies and data we presented here will serve as a useful starting point for those interested in conducting future prospective research on normal age-related changes in these structures.

References

1. Waller JM, Maibach HI: Age and skin structure and function, a quantitative approach (I): Blood flow, pH, thickness, and ultrasound echogenicity. Skin Res Technol 11:221, 2005
2. Machann J, Thamer C, Schnoedt B, et al: Age and gender related effects on adipose tissue compartments of subjects with increased risk for type 2 diabetes: A whole body MRI/MRS study. MAGMA Magnetic Resonance Materials in Physics, Biology and Medicine 18:128-137, 2005
3. Utzschneider KM, Carr DB, Hull RL, et al: Impact of intra-abdominal fat and age on insulin sensitivity and beta-cell function. Diabetes 53:2867-2872, 2004
4. Virtanen KA, Iozzo P, Hallsten K, et al: Increased fat mass compensates for insulin resistance in abdominal obesity and type 2 diabetes: A positron-emitting tomography study. Diabetes 54:2720-2726, 2005
5. Baumgartner RN, Rhyne RL, Troup C, et al: Appendicular skeletal muscle areas assessed by magnetic resonance imaging in older persons. J Gerontol 47:M67-72, 1992
6. Payne GW, Bearden SE: The microcirculation of skeletal muscle in aging. Microcirculation 13:275-277, 2006
7. Nair KS: Aging muscle. Am J Clin Nutr 81:953-963, 2005
8. Lubberink M, Tolmachev V, Widstrom C, et al: 110mIn-DTPA-D-Phe1-octreotide for imaging of neuroendocrine tumors with PET. J Nucl Med 43:1391-1397, 2002
9. Rabe JH, Mamelak AJ, McElgunn PJ, et al: Photoaging: Mechanisms and repair. J Am Acad Dermatol 55:1-19, 2006
10. Hashizume H: Skin aging and dry skin. J Dermatol 31:603-609, 2004
11. Kang S, Fisher GJ, Voorhees JJ: Photoaging: Pathogenesis, prevention, and treatment. Clin Geriatr Med 17:643-659, v-vi, 2001
12. Fisher GJ: The pathophysiology of photoaging of the skin. Cutis 75:5-8, 2005
13. Berardesca E, Maibach H: Ethnic skin: Overview of structure and function. J Am Acad Dermatol 48:139-142, 2003
14. Alaluf S, Atkins D, Barrett K, et al: Ethnic variation in melanin content and composition in photoexposed and photoprotected human skin. Pigment Cell Res 15:112-118, 2002
15. Kelly RI, Pearse R, Bull RH, et al: The effects of aging on the cutaneous microvasculature. J Am Acad Dermatol 33:749-756, 1995
16. Chung JH, Yano K, Lee MK, et al: Differential effects of photoaging vs intrinsic aging on the vascularization of human skin. Arch Dermatol 138:1437-1442, 2002
17. Fluhr JW, Elias PM: Stratum corneum pH: formation and function of the 'acid mantle'. Exogenous Dermatol 1:163-175, 2002
18. Wilhelm KP, Cua AB, Maibach HI: Skin aging. Effect on transepidermal water loss, stratum corneum hydration, skin surface pH, and casual sebum content. Arch Dermatol 127:1806-1809, 1991
19. Lavker RM, Zheng PS, Dong G: Aged skin: A study by light, transmission electron, and scanning electron microscopy. J Invest Dermatol 88:44s-51s, 1987 (suppl 3)
20. Gniadecka M: Effects of ageing on dermal echogenicity. Skin Res Technol 7:204-207, 2001
21. Hull MT, Warfel KA: Age-related changes in the cutaneous basal lamina: Scanning electron microscopic study. J Invest Dermatol 81:378-380, 1983
22. Branchet MC, Boisnic S, Frances C, et al: Skin thickness changes in normal aging skin. Gerontology 36:28-35, 1990
23. Sandby-Moller J, Poulsen T, Wulf HC: Epidermal thickness at different body sites: Relationship to age, gender, pigmentation, blood content, skin type and smoking habits. Acta Derm Venereol 83:410-413, 2003
24. Avram AS, Avram MM, James WD: Subcutaneous fat in normal and diseased states: 2. Anatomy and physiology of white and brown adipose tissue. J Am Acad Dermatol 53:671-683, 2005
25. Wajchenberg BL: Subcutaneous and visceral adipose tissue: Their relation to the metabolic syndrome. Endocr Rev 21:697-738, 2000
26. Kawashita NH, Brito MN, Brito SRC, et al: Glucose uptake, glucose transporter GLUT4, and glycolytic enzymes in brown adipose tissue from rats adapted to a high-protein diet. Metabolism 51:1501-1505, 2002
27. Truong MT, Erasmus JJ, Munden RF, et al: Focal FDG uptake in mediastinal brown fat mimicking malignancy: A potential pitfall resolved on PET/CT. AJR Am J Roentgenol 183:1127-1132, 2004
28. Barrington SF, Maisey MN: Skeletal muscle uptake of fluorine-18-FDG: Effect of oral diazepam. J Nucl Med 37:1127-1129, 1996
29. Johansson B: Brown fat: A review. Metabolism 8:221-240, 1959
30. Rodriguez-Cuenca S, Pujol E, Justo R, et al: Sex-dependent thermogenesis, differences in mitochondrial morphology and function, and adrenergic response in brown adipose tissue. J Biol Chem 277:42958-42963, 2002
31. Cohade C, Osman M, Pannu HK, et al: Uptake in supraclavicular area fat ("USA-Fat"): Description on 18F-FDG PET/CT. J Nucl Med 44:170-176, 2003
32. Yeung HW, Grewal RK, Gonen M, et al: Patterns of (18)F-FDG uptake in adipose tissue and muscle: a potential source of false-positives for PET. J Nucl Med 44:1789-1796, 2003

33. Baker GL: Human adipose tissue composition and age. Am J Clin Nutr 22:829-835, 1969
34. Kim S, Krynyckyi BR, Machac J, et al: Concomitant paravertebral FDG uptake helps differentiate supraclavicular and suprarenal brown fat uptake from malignant uptake when CT coregistration is not available. Clin Nucl Med 31:127-130, 2006
35. Hustinx R, Smith RJ, Benard F, et al: Dual time point fluorine-18 fluorodeoxyglucose positron emission tomography: A potential method to differentiate malignancy from inflammation and normal tissue in the head and neck. Eur J Nucl Med Mol Imaging 26:1345-1348, 1999
36. Gordon BA, Flanagan FL, Dehdashti F: Whole-body positron emission tomography: normal variations, pitfalls, and technical considerations. AJR Am J Roentgenol 169:1675-1680, 1997
37. Nakamoto Y, Higashi T, Sakahara H, et al: Delayed (18)F-fluoro-2-deoxy-D-glucose positron emission tomography scan for differentiation between malignant and benign lesions in the pancreas. Cancer 89:2547-2554, 2000
38. Lodge MA, Lucas JD, Marsden PK, et al: A PET study of 18FDG uptake in soft tissue masses. Eur J Nucl Med 26:22-30, 1999
39. Kumar R, Loving VA, Chauhan A, et al: Potential of dual-time-point imaging to improve breast cancer diagnosis with (18)F-FDG PET. J Nucl Med 46:1819-1824, 2005
40. Matthies A, Hickeson M, Cuchiara A, et al: Dual time point 18F-FDG PET for the evaluation of pulmonary nodules. J Nucl Med 43:871-875, 2002
41. Lardinois D, Weder W, Hany TF, et al: Staging of non-small-cell lung cancer with integrated positron-emission tomography and computed tomography. N Engl J Med 348:2500-2507, 2003
42. Pelosi E, Messa C, Sironi S, et al: Value of integrated PET/CT for lesion localisation in cancer patients: a comparative study. European Journal of Nuclear Medicine and Molecular Imaging 31:932-939, 2004
43. Antoch G, Saoudi N, Kuehl H, et al: Accuracy of whole-body dual-modality fluorine-18–2-fluoro-2-deoxy-d-glucose positron emission tomography and computed tomography (FDG-PET/CT) for tumor staging in solid tumors: comparison with CT and PET. J Clin Oncol 22:4357-4368, 2004
44. Hughes VA, Roubenoff R, Wood M, et al: Anthropometric assessment of 10-y changes in body composition in the elderly. Am J Clin Nutr 80:475-482, 2004
45. Cree MG, Newcomer BR, Katsanos CS, et al: Intramuscular and liver triglycerides are increased in the elderly. J Clin Endocrinol Metab 89: 3864-3871, 2004
46. Visser M, Pahor M, Tylavsky F, et al: One- and two-year change in body composition as measured by DXA in a population-based cohort of older men and women. J Appl Physiol 94:2368-2374, 2003
47. Kinahan PE, Hasegawa BH, Beyer T: X-ray-based attenuation correction for positron emission tomography/computed tomography scanners. Semin Nucl Med 33:166-179, 2003
48. Kirkland JL, Tchkonia T, Pirtskhalava T, et al: Adipogenesis and aging: does aging make fat go MAD? Exp Gerontol 37:757-767, 2002
49. Kirkeby S, Garbarsch C: Aging affects different human muscles in various ways. An image analysis of the histomorphometric characteristics of fiber types in human masseter and vastus lateralis muscles from young adults and the very old. Histol Histopathol 15:61-71, 2000
50. Dutta C, Hadley EC: The significance of sarcopenia in old age. J Gerontol A Biol Sci Med Sci 50 Spec No:1-4, 1995
51. Kirkeby S, Garbarsch C: Aging affects different human muscles in various ways. An image analysis of the histomorphometric characteristics of fiber types in human masseter and vastus lateralis muscles from young adults and the very old. Histol Histopathol 15:61-71, 2000
52. McCully KK, Posner JD: The application of blood flow measurements to the study of aging muscle. J Gerontol A Biol Sci Med Sci 50 Spec No:130-136, 1995
53. Frontera WR, Hughes VA, Fielding RA, et al: Aging of skeletal muscle: A 12-yr longitudinal study. J Appl Physiol 88:1321-1326, 2000
54. Janssen I, Heymsfield SB, Wang ZM, et al: Skeletal muscle mass and distribution in 468 men and women aged 18-88 yr. J Appl Physiol 89:81-88, 2000
55. Parkkola R, Kormano M: Lumbar disc and back muscle degeneration on MRI: Correlation to age and body mass. J Spinal Disord 5:86-92, 1992
56. Leroy-Willig A, Carlier P, Morvan D, et al: [Functional imaging of human muscle]. Rev Neurol (Paris) 154:379-388, 1998
57. Kemppainen J, Fujimoto T, Kalliokoski KK, et al: Myocardial and skeletal muscle glucose uptake during exercise in humans. J Physiol 542: 403-412, 2002
58. Bertoldo A, Pencek RR, Azuma K, et al: Interactions between delivery, transport, and phosphorylation of glucose in governing uptake into human skeletal muscle. Diabetes 55:3028-3037, 2006
59. Williams KV, Price JC, Kelley DE: Interactions of impaired glucose transport and phosphorylation in skeletal muscle insulin resistance: A dose-response assessment using positron emission tomography. Diabetes 50:2069-2079, 2001